Journal of Materials and Electronic Devices 2 (2025) 26-32

FYTRONIX JOURNAL OF MATERIALS AND ELECTRONIC DEVICES JMED http://dergi-fytronix.com/

PID Control of Proximal and Distal Interphalangeal Jointed Robotic Hand

Leyla Arslan[1], Muhammet Aydın[2,*]

[1]Firat University, Faculty of Engineering, Department of Mechatronics Engineering, Elazig, Turkiye
[2]Firat University, Faculty of Engineering, Department of Mechatronics Engineering, Elazig, Turkiye

This study presents the design, modeling, and control of a biomimetic robotic hand with independently actuated proximal (PIP) and distal (DIP) interphalangeal joints. A detailed anatomical reconstruction of the human hand was created in a CAD environment, where all finger joints were modeled as single-degree-of-freedom rotary joints. A total of 14 MG90S micro servo motors—three for each of the four fingers and two for the thumb—were integrated into the design to achieve a fully actuated, multi-input–multi-output (MIMO) structure capable of independent joint control.

Following the mechanical design, the model was transferred to a Python-based simulation environment, and PID controllers were implemented for MCP, PIP, and DIP joints. PID parameters were tuned and compared using Ziegler–Nichols and Cohen–Coon methods. Closed-loop angular responses of each joint were analyzed with respect to rise time, overshoot, damping ratio, and settling performance. The results show that while Ziegler–Nichols tuning provides rapid response, it introduces significant overshoot and oscillatory behavior, particularly in low-inertia joints such as the DIP. Conversely, the Cohen–Coon method yields more balanced, stable, and well-damped responses across all joints, making it a more suitable choice for robotic finger control where precise manipulation and stability are required.

This study demonstrates that a fully actuated robotic hand that adheres to anthropometric joint structures can successfully achieve natural finger motion using PID-based independent joint control. The findings provide an important foundation for future applications in prosthetics, rehabilitation robotics, and dexterous robotic manipulation.

Keywords: *Robotic hand, PID control, Ziegler-Nichols, Cohen-Coon.*

Submission Date: 09 August 2025
Acceptance Date: 18 November 2025

**Corresponding author:* muhammeta@firat.edu.tr

1. Introduction

The human hand, with its complex structure and functional flexibility, has been a focus of interest for many years, not only from a biomechanical perspective but also in engineering disciplines. The proximal and distal interphalangeal joints, which enable the fingers to move at different angles and axes, increase the hand's effectiveness in tasks requiring high coordination, such as grasping, holding, directing, and precise manipulation. Replicating this natural system in an artificial environment has been a critical research topic, particularly in recent years, in fields such as robotics, biomechanics, prosthetic technologies, and rehabilitation engineering.

Robotic hand designs are an important research topic in the fields of industrial automation and biomedical engineering. The complex structure and high functionality of the human hand are biomechanical properties that have long been attempted to be replicated in robotic systems. Therefore, realistic modeling of finger joints, accurate simulation of grasping dynamics, and the development of independent control structures are fundamental research areas that are constantly discussed in the literature.

Robotic hand design is not merely an effort to mechanically replicate a human hand; it is a multidisciplinary approach that integrates sensory feedback, control algorithms, and physical design. Reproducing the natural movements of a real human hand with an artificial system requires the flawless integration of high-precision control algorithms, the right choice of motors, and a design that conforms to human anatomy. However, in current studies, the detailed modeling of finger joints and the application of independent control systems for each joint are still limited.

In the literature, for practical reasons, the proximal interphalangeal (PIP) and distal interphalangeal (DIP) joints are often kinematically coupled, while the independent modeling of all finger joints (metacarpophalangeal (MCP), PIP, DIP) remains limited [1,2]. In this study, however, the natural range of motion, rotation axes, and connection types for each joint were considered separately; the design and control architecture were created according to these details. Thus, the study complies with biomimetic design principles and offers a solution that balances the two extremes in the literature with an independent servo motor and PID-based control approach.

In this study, the joints of the robotic hand, modeled in SolidWorks according to anatomical proportions, were defined as single-degree-of-freedom rotary joints. Subsequently, a total of 14 servo motors were added—three for each of the four fingers and two for the thumb—to create an independently drivable Multiple Input Multiple Output (MIMO) control structure. In the final stage, the model was transferred to a Python-based simulation environment; the joint moment–position relationships were evaluated using PID control, and the PID coefficients were optimized using the Ziegler–Nichols and Cohen–Coon methods. Thus, the kinematic and control performance of the joints were tested, and the opening–closing behaviors of the robotic hand were analyzed.

1.1. History and development process of robotic hand systems

The development of robotic hand systems is the result of long-term efforts to replicate the complex biomechanical structure of the human hand using engineering methods. Among the first agile hand prototypes, the Stanford/JPL Hand and Utah/MIT Dextrous Hand were developed in the 1980s to investigate fundamental grasping dynamics such as multi-joint coordination, force control, and fingertip interaction [3]. These early studies laid the groundwork for subsequent generations of robotic hand designs. From the 1990s to the 2010s, an evolution from laboratory prototypes to more application-ready systems was observed. The DLR-Hand II stood out with its integrated actuator modules, advanced sensory feedback capabilities, and multi-degree-of-freedom finger kinematics [4]. Similarly, the BarrettHand (BH8 series) became a widely accepted platform in practice due to its compact design and easy integration with industrial robots [5].

In the 2010s, cost, durability, and simplicity of control came to the forefront in robotic hand design; underactuated and soft robotics approaches matured. In particular, Pisa/IIT SoftHand, with its adaptive synergy design that enables the coordinated movement of all fingers with a single actuator, has provided an important threshold in mimicking the biological grasping patterns of the human hand [6]. During the same period, flexible materials and tendon-driven actuation architectures have enabled the development of more harmonious and safer systems in human-robot interaction.

Since 2018, machine learning and, in particular, reinforcement learning-based control approaches have come to the fore in robotic hand systems. Learning-based control frameworks developed on the Shadow Dexterous Hand have enabled the transfer of in-hand manipulation capabilities from the simulation environment to the physical system through simulation-to-real strategies supported by comprehensive domain randomizations [7].

In the post-2020 period, significant progress has been made in robotic hand designs in terms of integration, low cost, and manufacturability. For example, the ILDA (Integrated Linkage Driven Anthropomorphic) hand design integrates actuator and sensor components into the palm, offering meaningful gains in compactness, force generation, and agility [8]. At the same time, the ability to produce models such as BRL/Pisa/IIT SoftHand entirely through 3D printing has contributed to reducing costs and shortening prototype development times [6].

During this period, fingertip tactile sensor integration also came to the fore in advanced versions of Shadow Dexterous Hand systems, becoming a component that enhances the system's adaptation and precision control capabilities in grasping scenarios requiring tactile feedback [9].

1.2. The Bony and Joint Structure of the Human Hand

The human hand is a complex structure composed of carpal, metacarpal, and phalangeal bones. The 2nd–5th fingers have MCP, PIP, and DIP joints, while the thumb has MCP and IP joints. MCP joints have a condyloid (biaxial) structure and two degrees of freedom; PIP and DIP joints are hinge-type joints that primarily allow flexion/extension [10]. Figure 1 demonstrates the joints of the human hand.

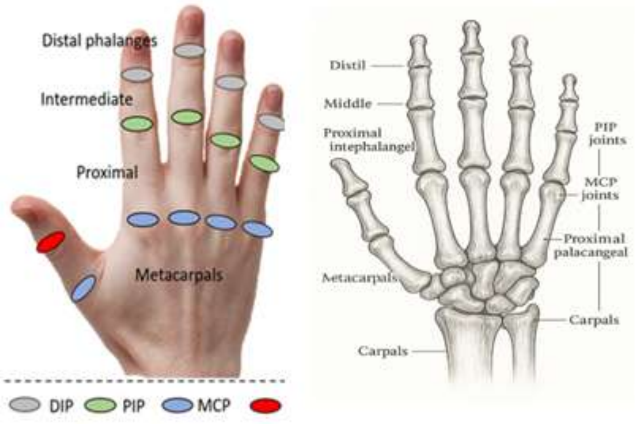

Fig.1. The joint structure of the human hand

Joint stability is provided by the collateral ligaments, the palmar plate, and the dorsal extensor mechanism. In particular, the oblique retinaculum ligament (ORL) and the transverse retinaculum ligament (TRL) support coordination between the finger joints by regulating the movement coupling between the PIP and DIP joints [11].
Kinematics studies show that there is a near-linear (approximately constant ratio) relationship between DIP and PIP joint angles; DIP movement generally ranges between approximately 0.7–0.8 relative to PIP [14]. In terms of range of motion, MCP flexion has been reported to be approximately 85–90°, PIP approximately 95°, and DIP approximately 80–85° [14]. Functional range of motion (FROM) indicates that lower subranges of these maximums are used in activities of daily living [12-13].

2. Material and Methods

2.1. Basic Hand Model Designed Prior to Motor Integration

At this stage, a preliminary mechanical design based on the morphology of the human hand has been created in a CAD environment. The goal is to obtain a skeleton that is compatible with anthropometric ratios, kinematically correct, and capable of integrating servo motors and transmission elements in the future. This phase focuses solely on geometric and kinematic accuracy; material assignments, flexibility/friction effects, and structural analyses are excluded. Figure 2 shows the robotic hand created for this phase.

Fig.2. Robotic hand model developed prior to motor integration

The assembly strategy was based on top-down parameterization; first, the joint axes and finger segment ratios were defined, then the phalanges and joint blocks were created parametrically. In the assembly, all joints are defined as ideal revolute joints, with assigned angle limits and kinematic integrity verified through collision/freedom checks. This model serves as a kinematic skeleton that will be used as a reference for future servo motor integration and transmission architecture additions.
Metacarpophalangeal (MCP) joints: These condyloid joints, in addition to flexion–extension (bending–straightening), also allow abduction–adduction (moving away from and toward the hand's midline). In the human hand, MCP joints have approximately two degrees of freedom.
Proximal interphalangeal (PIP) joints: These are hinge-type joints that allow only flexion and extension. They have a single degree of freedom.
Distal interphalangeal (DIP) joints: Similar to the PIP joints, these are hinge-type joints that perform flexion and extension with a single degree of freedom.
The thumb, however, has a joint structure different from the other fingers. The thumb has a metacarpophalangeal (MCP) joint and an interphalangeal (IP) joint. Although the MCP joint can exhibit partially multi-axial motion, it is generally modeled as a single–degree-of-freedom hinge. The IP joint is a single-DoF hinge that performs flexion–extension.
Accurately modeling these joint types in robotic designs increases both the naturalness of finger movements and the reliability of grasp tasks. As shown in Figure 2, correctly modeling the positions of the MCP, PIP, and DIP joints as in the human hand is of critical importance, especially for precise manipulation and human-like grasping capability.

2.2. Motor Selection and Suitability of the Motor Used

Motor selection in robotic hand design is a critical design step that directly affects the performance and biomechanical integrity of the mechanism. In this context, motors have been evaluated based on their output torque, physical dimensions, and dynamic response characteristics. For the fingers to safely generate the required grasping force on an object, the motor must have sufficient output torque. Insufficient torque both reduces gripping stability and negatively affects the accuracy of modeling results. In addition, motors must be integrated into the palm and finger modules without creating additional volume in order to preserve the anatomical form similar to the human hand. Since oversized motors disrupt this integrity, compact and lightweight servo models have been preferred. Furthermore, it is important that the motors offer sufficient angular speed and fast dynamic response characteristics so that finger movements can occur at speeds close to natural hand dynamics; low speeds can cause delays in the manipulation process, while excessively high speeds can lead to control instability.

In line with these requirements, the MG90S micro servo motor was used in the study. The motor's compact dimensions (22.8 × 12.2 × 28.5 mm) and low mass (~13 g) provide a significant advantage for applications requiring limited volume in biomechanical hand designs. Capable of producing stall torques of 2.2 kg·cm and 2.5 kg·cm at operating voltages of 4.8–6.0 V, respectively, the MG90S has the capacity to meet the torque requirements of finger joints. Furthermore, its speed performance of 0.10–0.12 s/60° and maximum rotation angle of approximately 180° align with the targeted motion ranges of finger joints connected to the four-bar mechanism, demonstrating its ability to meet ROM (Range of Motion) requirements.

The metal gear structure of the motor offers higher durability compared to plastic gears and reduces the risk of deformation under repeated loads. Its low weight contributes to the design remaining biomechanically balanced by not adding extra load to the system's total mass. Furthermore, the 4.8–6.0 V operating range is directly compatible with the microcontroller and power unit used, eliminating the need for an additional converter.

Considering all these technical specifications, the MG90S micro servo motor is suitable as an actuator compatible with the kinematic structure, torque requirements, and control strategies of the designed robotic hand.

In this study, a separate servo motor was assigned to each joint to enable the finger joints to produce independent movements similar to those of the human hand. This approach allows for precise control of joint movements, enabling the creation of a multi-input–multi-output (MIMO) drive architecture. For the four main fingers (index, middle, ring, and pinky), each of the MCP, PIP, and DIP joints was driven independently, using a total of 12 motors. In accordance with the anatomy of the thumb, two independent motors were added for the MCP and IP joints, thus positioning a total of 14 MG90S micro servos in the system. The placement of the motors close to the relevant joints has reduced mechanical backlash and increased the accuracy of motion transmission. This fully actuated structure, unlike the partially actuated mechanisms in the literature, allows the fingers to move independently but produce coordinated movements when necessary.

2.3. Servo Motor Placement, Capacity Suitability, and Joint Angle Limits

The angular motion obtained from the servo shaft is transferred to the joint axes via a four-bar linkage mechanism (servo arm–linkage rod–rocker). This solution was chosen for its packaging flexibility and adjustable transmission ratio. The torque capacities of the motors are sufficient to meet the forces required during gripping. The joint limits defined in the CAD environment are set as MCP 0–90°, PIP 0–100°, DIP 0–80°, thumb MCP 0–60°, and IP 0–80°. These limits are consistent with anthropometric data and ensure kinematic integrity. The limit ranges have been verified with Clearance/Interference checks, and Motion Study analyses have demonstrated the repeatability of the kinematic profile. Furthermore, the approximately 180° rotation capacity of the MG90S servo motors used exceeds the joint ROM requirements, and thanks to their transmission ratios, the targeted movement ranges for each joint have been achieved without loss. Figure 3 shows the robotic hand with the motors installed.

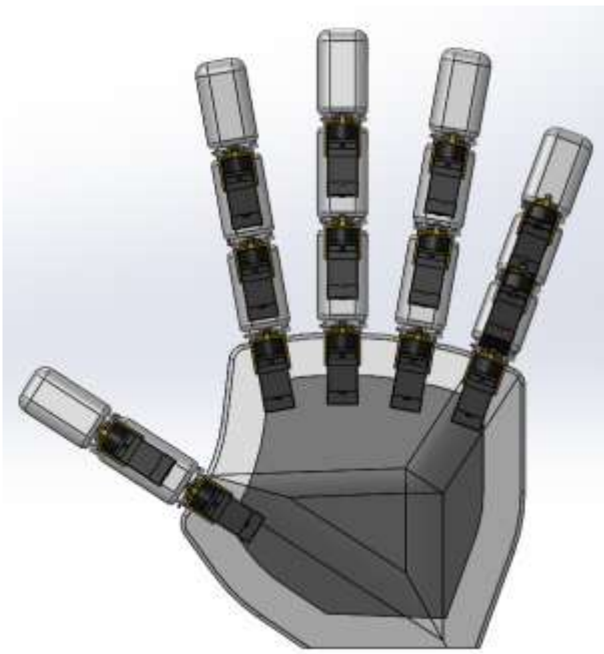

Fig.3. View of robotic hand with motor placed on it

2.4. Closed-Loop Performance Analysis of PID Tuning Methods

In this section, PID controllers for the three joints of the robotic finger (MCP, PIP, and DIP) were tuned using the Ziegler–Nichols (ZN) and Cohen–Coon (CC) methods; then, the closed-loop angular response behavior of each joint was analyzed. The objective is to determine which method produces a more balanced, more stable, and less overshoot response for each joint.

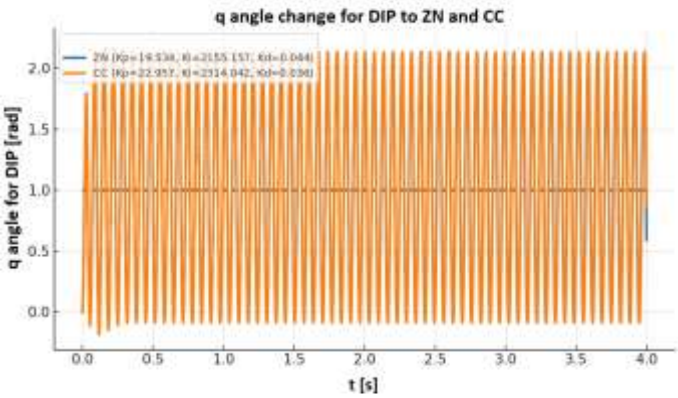

Fig.4. The closed-loop q angle graph for DIP joint

Three different closed-loop graphs were obtained during the analyses. These graphs are presented in Figure 4 for the DIP joint, Figure 5 for the MCP joint, and Figure 6 for the PIP joint, respectively.
Figure 4 indicates that the gain coefficients in the ZN method are Kp=19.534, Ki=2155.157, Kd=0.044; while the gain coefficients in the CC method are Kp=22.957, Ki=2314.042, Kd=0.036.

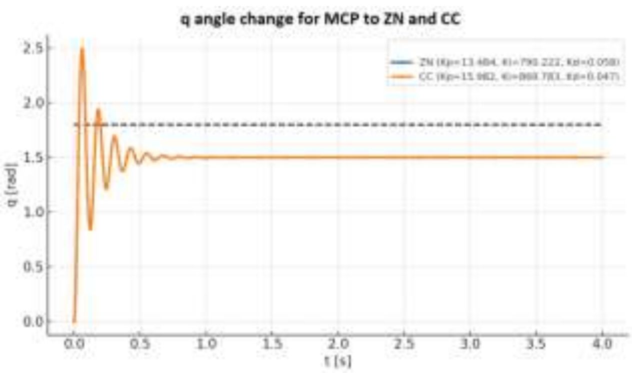

Fig.5. The closed-loop q angle graph for MCP joint

According to Figure 5, the ZN method's gain coefficients are Kp=13.484, Ki=790.222, and Kd=0.058, whereas the CC method's gain coefficients are Kp=15.982, Ki=869.783, and Kd=0.047.

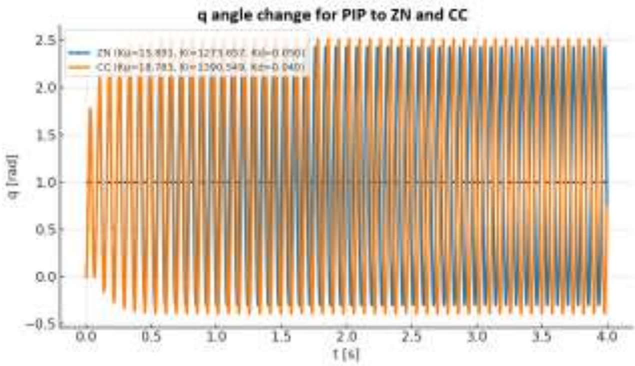

Fig.6. The closed-loop q angle graph for PIP joint

The ZN method's gain coefficients are Kp=15.891, Ki=1273.657, and Kd=0.050; the CC method's gain coefficients are Kp=18.783, Ki=1390.549, and Kd=0.040, as shown in Figure 6.

3. Results and Discussion

Figure 4 displays the closed-loop behavior of the MCP joint. The MCP joint is the joint with the highest inertia and lowest stiffness coefficient in the robotic finger. Due to the MCP joint being the heaviest joint, the closed-loop response time is significantly slower compared to the other two joints. The ZN behavior caused a rapid rise in the MCP; however, noticeable overshoot, long settling time, and low damping were observed. Due to integrator accumulation, windup symptoms were observed in the form of short-term oscillations. The attitude towards CC behavior produced a softer response in the MCP, with low overshoot and shorter settling time. Although the initial rise is slower than with ZN, the overall system stability is better. Consequently, CC is more balanced in the MCP joint. If ZN is to be used: Kp should be reduced by 10–20%, Ki should be decreased by 10–15%, and Kd should be slightly increased.
Figure 5 presents the closed-loop angular response of the PIP joint. The PIP joint is positioned between the MCP and DIP joints in terms of stiffness, velocity, and inertia. The PIP joint is a medium-velocity and medium-stiffness joint; its response velocity is reasonable, and its movement smoothness is average. The ZN setting produced high initial acceleration in the PIP joint; however, moderate overshoot and prolonged settling time were observed. The single/double-peaked slight oscillations seen in the graphs indicate that the PIP exhibited more aggressive behavior under ZN. The CC setting produced a significantly more controlled response in the PIP joint, with low overshoot and a short settling time. As a result, CC generally produces a cleaner closed loop in the PIP joint. If ZN is to be used, Ki should be reduced slightly, and Kd should be increased by 10–15%.
Figure 6 depicts the closed-loop response of the DIP joint. The DIP joint is the lightest and fastest joint in the robotic

finger. Due to its low inertia, the DIP joint produces the fastest angular response. The ZN method setting produced a highly aggressive response in the DIP joint. Although the rise time is very short, overshoot is pronounced, damping is weak, and high-frequency short oscillations are observed. If the moment limits are exceeded, saturation-induced peak behaviors may occur. The CC method produced a calmer, lower overshoot, and cleaner settling response in this joint. Although the rise speed is lower than ZN, the damping is better. In conclusion, for daily use, CC offers a more stable and lower overshoot option for DIP. If ZN is to be used, to limit overshoot: Ki should be reduced, Kd should be increased.

When the PID comparisons for the three joints of the robotic hand are evaluated together, the overshoot amount is mostly due to the controller's insufficient damping, the high proportional gain, and the dynamics related to joint inertia. Especially for the MCP, which has high inertia, high Kp values tend to cause excessive overshoot in this joint. The analyses show that the Cohen–Coon method in PID control of robotic finger joints provides a more balanced, stable, and smoothly damped closed-loop performance across all joints. Although the Ziegler–Nichols method is fast to tune, it creates undesirable effects such as high overshoot, oscillation, and prolonged settling time. Consequently, unless speed is a primary requirement in robotic finger designs, the CC method should be considered a more reliable choice.

4. Conclusion

In this study, a fully actuated robotic hand system was designed, modeled, and analyzed based on the biomechanical structure of human finger joints. Each joint was independently driven using MG90S servo motors, allowing the robotic hand to perform natural, human-like finger motions with high controllability. The mechanical model was verified through kinematic analyses, and the independent joint architecture established a robust platform for closed-loop control.

PID controllers were applied to the MCP, PIP, and DIP joints, and the tuning performance of Ziegler–Nichols and Cohen–Coon methods was comparatively evaluated. Across all joints, Cohen–Coon tuning produced smoother transitions, lower overshoot, and faster settling, whereas Ziegler–Nichols tuning—despite its fast rise time—resulted in oscillations and insufficient damping. These findings indicate that for applications requiring precise and stable finger control, the Cohen–Coon method is the more appropriate tuning strategy.

Overall, the proposed robotic hand design successfully combines anatomical accuracy, independent actuation, and optimized control performance. The study contributes a realistic and controllable robotic hand architecture that can serve as a foundational platform for advanced manipulation tasks, prosthetic device development, and future intelligent control strategies such as adaptive control or learning-based joint optimization.

Acknowledgments
This study was produced from studies carried out within the scope of the first author's master's thesis topic.

References

[1] Deimel, R. and Brock, O., A novel type of compliant and underactuated robotic hand for dexterous grasping, The International Journal of Robotics Research, 35:1–3 (2016) 161–185. https://doi.org/10.1177/0278364915592961.

[2] Grazioso, A., Potenza, D.C., Zappatore, G.A. and Reina, G., Performance analysis of the underactuated finger for Adam’s Hand, IEEE Access, 12 (2024) 33456–33468. https://doi.org/10.1109/ACCESS.2024.3477249.

[3] Piazza, C., et al., A century of robotic hands, Annual Review of Control, Robotics, and Autonomous Systems, 2 (2019) 1–32. https://doi.org/10.1146/annurev-control-060117-105003.

[4] Grebenstein, M., Chalon, M., Friedl, W., Haddadin, S., Wimböck, T., Hirzinger, G. and Siegwart, R., The hand of the DLR hand arm system: Designed for interaction, The International Journal of Robotics Research, 31:13 (2012) 1531–1555. https://doi.org/10.1177/0278364912459209.

[5] Townsend, W., The BarrettHand grasper–programmably flexible part handling and assembly, Industrial Robot: An International Journal, 27:3 (2000) 181–188. https://doi.org/10.1108/01439910010371597.

[6] Catalano, M.G., Grioli, G., Farnioli, E., Serio, A., Piazza, C. and Bicchi, A., Adaptive synergies for the design and control of the Pisa/IIT SoftHand, The International Journal of Robotics Research, 33:5 (2014) 768–782. https://doi.org/10.1177/0278364913518995.

[7] Andrychowicz, O.M., Baker, B., Chociej, M., Jozefowicz, R., McGrew, B., Pachocki, J., … and Zaremba, W., Learning dexterous in-hand manipulation, The International Journal of Robotics Research, 39:1 (2020) 3–20. https://doi.org/10.1177/0278364919888756.

[8] Kim, U., Jung, D., Jeong, H., Park, J., Jung, H.M., Cheong, J., … and Park, C., Integrated linkage-driven dexterous anthropomorphic robotic hand, Nature Communications, 12 (2021) 7177. https://doi.org/10.1038/s41467-021-27261-0.

[9] Huang, Y., Fan, D., Duan, H., Yan, D., Qi, W., Sun, J., and Wang, P., Human-like dexterous manipulation for anthropomorphic five-fingered hands: A review, Biomimetic Intelligence and

Robotics, 5:1 (2025) 100212. https://doi.org/10.1016/j.birob.2025.100212.
[10] Leijnse, J.N.A.L., Quesada, P.M. and Spoor, C.W., Kinematic evaluation of the finger's interphalangeal joints coupling mechanism—variability, flexion–extension differences, triggers, locking swanneck deformities, anthropometric correlations, Journal of Biomechanics, 43:12 (2010) 2381–2393. https://doi.org/10.1016/j.jbiomech.2010.05.030.
[11] Balakrishnan, T.M., Subbaraj, H. and Jaganmohan, J., Anatomy of Landsmeer ligaments—redefined, Indian Journal of Plastic Surgery, 52:2 (2019) 195–200. https://doi.org/10.1055/s-0039-1695802.
[12] Yatağan, K.M., Biomechanical Modelling of the Interphalangeal Joints of the Human Hand, Master's Thesis, Middle East Technical University, Turkey, (2021).
[13] Gracia-Ibáñez, V., Vergara, M., Sancho-Bru, J.L., Mora, M.C. and Piqueras, C., Functional range of motion of the hand joints in activities of the International Classification of Functioning, Journal of Hand Therapy, 30:3 (2017) 337–347. https://doi.org/10.1016/j.jht.2017.01.009.